JOURNAL OF MATERIALS SCIENCE 27 (1992) 504–510

Age-hardening associated with ordering and spinodal decomposition in a AgCu–40 at % Au pseudobinary alloy

KOH-ICHI UDOH, HIROYUKI FUJIYAMA*, KUNIHIRO HISATSUNE, MASAYUKI HASAKA*, KATSUHIRO YASUDA
Department of Dental Materials Science, Nagasaki University School of Dentistry, 7-1 Sakamoto-machi, Nagasaki 852, Japan
**Department of Materials Science and Engineering, Faculty of Engineering, Nagasaki University, 1-14 Bunkyo-machi, Nagasaki 852, Japan*

The age-hardening mechanism in an AgCu–40 at % Au alloy was studied by means of electrical resistivity measurement, hardness tests, X-ray diffraction and electron microscopy. Two stages of hardening were found by isothermal ageing below 648 K, which was higher than the critical temperature of ordering, T_c = 620 K, in the present alloy. The first stage of hardening took place by formation of a modulated structure resulting from spinodal decomposition. Further hardening was brought about by ordering, yielding metastable AuCu I′ and/or AuCu II′ ordered platelets grown from the copper-rich portion of the modulated structure. Transitional ordering which gave rise to a marked hardening of the second stage was found, even though the temperature of below 648 K was higher than the T_c of the present alloy. Drastic softening was also found on disappearance of the transitional ordered phases. Although the modulated structure was observed by ageing at 773 K, there was no age-hardening.

1. Introduction

It has been well known that the ternary system Au–Cu–Ag is characterized by ordering and a two-phase decomposition, and shows significant age-hardening in a certain composition region. Previous work has shown that aged Au–49.8 at % Cu–15.7 at % Ag (14 K) [1, 2] and Au–55.2 at % Cu–17.4 at % Ag (12 K) [3] alloys exhibit X-ray diffraction patterns of "side-bands" which are associated with spinodal decomposition. Electron micrographs of these alloys in a lower ageing temperature range show a fine mottled contrast parallel to the ⟨1 0 0⟩ directions in the early stage of ageing. This fine contrast is due to the formation of a modulated structure induced by spinodal decomposition, which is confirmed by the appearance of side-bands in X-ray diffraction patterns and satellite reflections around fundamental reflections in the electron diffraction patterns.

It is supposed that the age-hardening characteristics of Au–Cu–Ag ternary alloys are affected by their compositions, especially by the atomic ratio of gold to copper. Because the tendency for two-phase decomposition markedly increases with decreasing gold content, the effect of the ordered phase on age-hardening may diminish or disappear altogether. Therefore, the present study is conducted to elucidate the sequence of phase transformation associated with age-hardening in a low gold-content alloy, in which the ratio of copper to silver is maintained equiatomic, using X-ray and electron diffraction, transmission electron microscopy, electrical resistivity measurements and hardness tests.

2. Experimental procedure

An alloy which contained 40 at % Au, 30 at % Cu and 30 at % Ag was prepared by vacuum-melting in a high-frequency induction furnace. The alloying constituents used were 99.99% purity materials. To ensure uniformity of composition, the alloy ingot was swaged a little and homogenized at 973 K for 7.2 ks under an argon atmosphere, and then quenched into ice brine.

Test-pieces for hardness tests were cold-rolled into 5 mm × 5 mm × 1 mm sheets. The measurements were made on test-pieces after being subjected to various temperatures and periods of ageing, using a 0.98 N load and a diamond pyramid indentor. Discs 3 mm in diameter punched out from strips that had been cold-rolled to a thickness of 0.1 mm were electro-thinned by a double-jet technique for examination by transmission electron microscopy (TEM) after being subjected to the required heat treatment. The electrolyte used for this thinning was prepared by dissolving 35 g of chromium trioxide in a solution of 200 ml acetic acid and 10 ml distilled water. A 200 kV electron microscope equipped with a specimen tilting device was employed in the present study. Resistivity was

0022–2461/92 $03.00 + .12

measured by a potentiometric method on a solution-treated strip during continuous heating and cooling from room temperature to 973 K and vice versa at a constant rate of 1.7×10^{-3} K s^{-1}. Powder specimens for X-ray diffraction study were vacuum-sealed in a silica tube and subjected to heat treatment at required temperatures and periods.

3. Results

3.1. Electrical resistivity

Fig. 1 shows the ageing behaviour of the solution-treated and quenched alloy examined by the heating excursion of electrical resistivity measurement. Curve (a) demonstrates the resistivity change which is represented by the ratio of resistivity at a measured temperature and at the disordered temperature (973 K). The resistivity increases with temperature, starts to decrease at around 370 K reaches a minimum value at about 500 K and then rises to a relatively higher value at 666 K after showing a slight swelling at approximately 630 K. An appreciable inflection can be seen at a temperature of 875 K in curve (a). During the cooling process, the resistivity dropped at about 575 K after showing a slight inflection at around 795 K, and then decreased in proportion to the temperature decrease. Although hysteresis is observed, the mean value of the inflection points, 835 and 620 K, are determined to be the phase transformation temperatures in the present alloy. This determination seems to be reasonable on the basis of the observation by means of TEM as will be shown later.

Curve (b) in Fig. 1 shows the temperature derivative curve of the heating process which is obtained by plotting values of $d\rho/dT$ between pairs of adjacent points in curve (a) against the temperatures midway between each pair. There are clearly visible a vague peak and sharp double peaks. The latter exhibits the λ-shape peak which is characteristic of order–disorder transformation and the double peak suggests a complex ordering process. Thus, these resistivity changes in the present alloy can be regarded as AuCu I and AuCu II ordering (620 K) and a two-phase decomposition (835 K), as will be shown later.

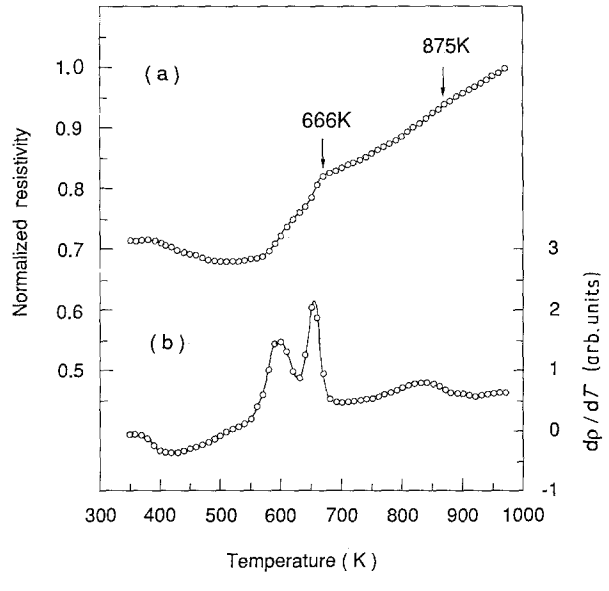

Figure 1 Changes in (a) the electrical resistivity and (b) its temperature derivative, plotted against the ageing temperature.

3.2. Age-hardening characteristics

Fig. 2 shows the variation of hardness during isothermal ageing at several constant temperatures. It is observed that significant age-hardening occurs below 648 K, even though this temperature is higher than the critical temperature of ordering, 620 K, determined from resistivity. Below a temperature of 648 K, the age-hardening curves demonstrate a two-stage hardening, i.e. the curves start to increase in hardness at the initial stage of ageing as indicated by single arrows, go through a slight decrease in hardness and then rise to maximum hardness as shown by double arrows. A marked softening is observed in the hardening curves after lengthy ageing periods. When the specimen is aged at 773 K for an extended period, there is no hardening as seen in Fig. 2.

Thus, it is suggested from the age-hardening behaviour in the present alloy that two-phase transformation associated with hardening takes place depending on the temperature.

3.3. X-ray diffraction

To elucidate the sequence of phase changes during isothermal ageing, X-ray diffraction patterns were taken from specimens aged for various periods at 523–773 K. Fig. 3 represents the 1 1 1 and 2 0 0 fundamental reflections of specimens aged at 773 K for the periods indicated. The solution-treated specimen (S.T.), which is designated as α_0 phase, gives an X-ray diffraction pattern of the face-centred cubic (f.c.c.) lattice which possesses a lattice parameter $a = 0.3959$ nm. Two sets of diffraction peaks for the f.c.c. lattice which are designated as α_1 and α_2 phases appear in the diffraction patterns during ageing. No superlattice reflections were observed at the positions expected in the X-ray diffraction pattern. The lattice parameters of the α_1 and α_2 phases were calculated to be $a(\alpha_1) = 0.3879$ nm and $a(\alpha_2) = 0.4034$ nm, respectively. Therefore, it is suggested that a two-phase decomposition takes place during the later stage of ageing at 773 K.

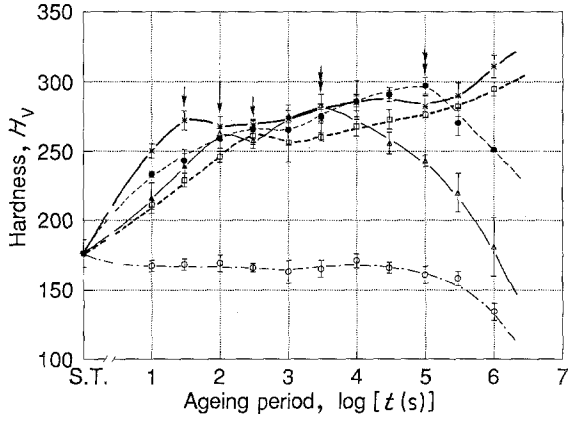

Figure 2 Isothermal age-hardening curves of alloy solution-treated at 973 K: (□) 523 K, (∗) 573 K, (●) 623 K, (△) 648 K, (○) 773 K.

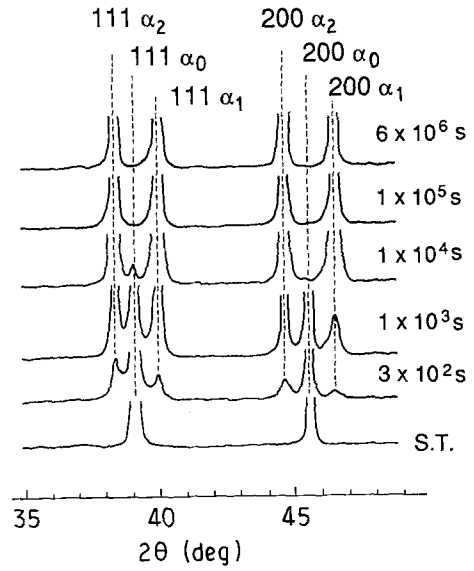

Figure 3 Changes in X-ray diffraction profiles of the 1 1 1 and 2 0 0 reflections during isothermal ageing at 773 K for various periods.

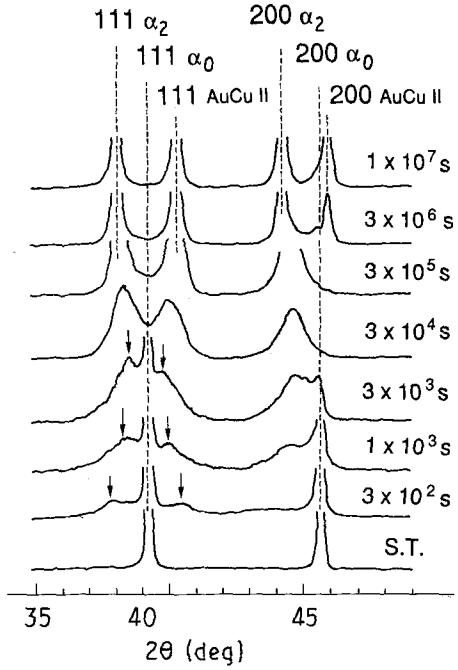

Figure 4 Changes in X-ray diffraction profiles of the 1 1 1 and 2 0 0 reflections during isothermal ageing at 573 K for various periods.

On the other hand, quite different changes in X-ray diffraction patterns were observed by ageing below 648 K. Fig. 4 shows the 1 1 1 and 2 0 0 fundamental reflections of a specimen aged at 573 K for the periods indicated in the figure. Although two-phase decomposition occurs from the α_0 phase, an apparent shift of diffraction peaks of the α_1 and α_2 phases is observed during a relatively early stage of ageing. This will be caused by variation in composition of these phases during ageing at 573 K, and provides evidence against a homogeneous mechanism of two-phase decomposition. The discontinuous process is also brought about in the later stage of ageing.

It seems that side-bands accompany the 1 1 1 reflection of the α_0 phase in the early stage, as indicated by arrows in Fig. 4. With the progress of ageing, the side-bands move closer to the main reflection. These changes suggest formation of a modulated structure resulting from spinodal decomposition, as observed in the 14 K [1] and 12 K [3] Au–Cu–Ag ternary alloys. However, it is strange that the side-bands could not be found around the 2 0 0 fundamental reflection of the α_0 phase in Fig. 4. This may be thought to show that the spinodal decomposition is generated immediately, followed by initiation of the AuCu ordering below 620 K. Actually, formation of the modulated structure was observed in TEM micrographs. Satellite reflections or side-maxima were also found around the fundamental reflections in selected-area electron diffraction (SAED) patterns, as will be shown later.

Fig. 5 represents changes in the X-ray diffraction profile of the 0 0 1 and 1 1 0 superlattice reflections during ageing at 573 K for various periods. Superlattices formed in the present alloy are identified to be metastable AuCu I′ with f.c.t. structure, metastable AuCu II′ with long-period superstructure, stable AuCu I and stable AuCu II ordered phases. The Miller indices used here are expressed as for domain size $M = 5$ according to Johansson and Linde [4]. Although the superlattice reflections for the metastable AuCu I′ and AuCu II′ phases become more distinguishable by ageing, these metastable ordered phases are extinguished with further ageing, and a stable AuCu II ordered phase is observed with a stable α_2 phase. It should be noted that the stable AuCu I ordered phase is not formed by ageing at 573 K.

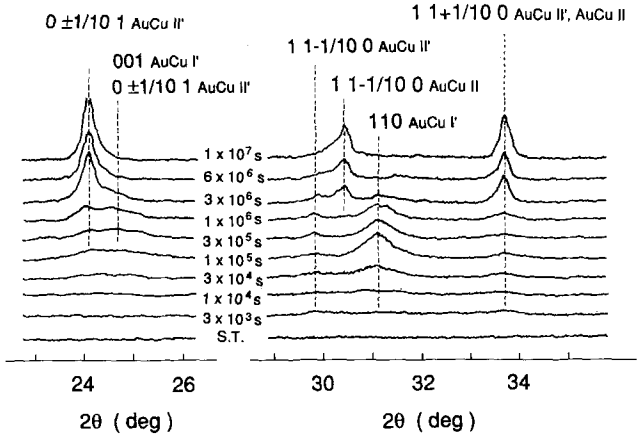

Figure 5 Changes in X-ray diffraction profiles of the 0 0 1 and 1 1 0 superlattice reflections during isothermal ageing at 573 K for various periods.

Thus, the phase transformation sequence at 573 K is described from the results obtained by the X-ray diffraction study as follows. The disordered solid solution, α_0, is decomposed by spinodal decomposition at first, and the modulated structure is formed. The copper-rich portion of the modulated structure then changes to the metastable AuCu I′ and AuCu II′ ordered phases, while the silver-rich portion becomes a metastable α_2' phase by a continuous mechanism. Finally, the stable AuCu II ordered and α_2 phases are formed by a discontinuous mechanism. A similar phase transformation sequence was found in changes of the X-ray diffraction patterns during ageing at 603 K.

By ageing at 523 K, the modulated structure was brought about by spinodal decomposition in the early

stage of ageing. Then, the metastable AuCu I′ ordered and metastable α_2' silver-rich phases were formed by a continuous mechanism. With further ageing, these metastable phases changed into the stable AuCu I ordered and the α_2 phases by a discontinuous mechanism.

It was also found that transitional ordering was extinguished finally by ageing in a certain temperature range. Fig. 6 shows the changes in X-ray diffraction profiles in the vicinity of the 0 0 1 and 1 1 0 superlattice reflections for samples aged at 623 K for the periods indicated. It is clearly visible that the superlattice reflections for the metastable AuCu I′ and AuCu II′ phases become more intense during the middle stage of ageing. However, these metastable ordered phases are extinguished with further ageing. The final structure consisted of the α_1 and α_2 equilibrium phases.

3.4. TEM observations

Fig. 7a and b show the dark-field TEM image and SAED pattern, respectively, taken from a specimen aged at 773 K for 3×10^2 s. The dark-field image is produced by using the 2 2 0 fundamental reflection to enhance the cross-hatched contrast by making traces parallel to the ⟨1 0 0⟩ directions, as seen in Fig. 7a. In the SAED pattern, characteristic side-maxima are visible along the ⟨1 0 0⟩ directions. The appearance of the cross-hatched contrast and side-maxima indicate the formation of periodic variations of the lattice parameter and an atomic scattering factor caused by the periodic composition fluctuation along ⟨1 0 0⟩ directions, i.e. the formation of the modulated structure. There is no doubt that the TEM micrograph and SAED pattern show the formation of the modulated structure resulting from spinodal decomposition, although the spinodal decomposition occurs so rapidly in the early stage of ageing that the side-bands were not observed in X-ray diffraction profiles of the fundamental reflections aged at 773 K (Fig. 3). With further ageing, no ordered phases were found in SAED patterns.

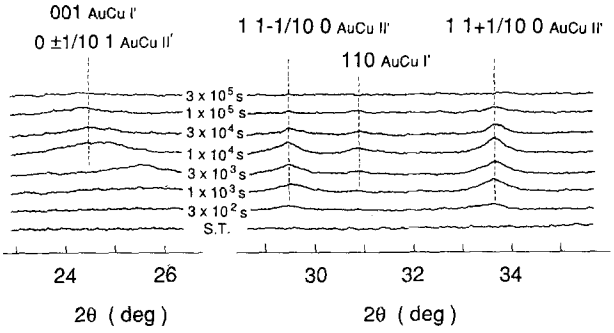

Figure 6 Changes in X-ray diffraction profiles of the 0 0 1 and 1 1 0 superlattice reflections during isothermal ageing at 623 K for various periods.

Fig. 8a and b represent respectively the dark-field image formed by using the 2 2 0 fundamental reflection and the SAED pattern, taken from a specimen aged at 573 K for 1×10^2 s. The configuration of the TEM image is completely the same as that of Fig. 7a. As was demonstrated by the X-ray diffraction study (Figs 4 and 5), the copper-rich portion of the modulated structure altered to the metastable AuCu I′ and AuCu II′ ordered phases.

Fig. 9 shows TEM micrographs and an SAED pattern taken from a specimen aged at 573 K for 10 ks. In the SAED pattern shown in Fig. 9d, superlattice reflections are found at the position of the 0 0 1, 1 1 0 and equivalent positions. Moreover, these superlattice reflections are separated into two or four spots. This suggests the formation of an $L1_0$-type superlattice of the AuCu I and of a periodic antiphase domain structure of the AuCu II ordered phases, corresponding to the metastable phases suggested by the X-ray diffraction study. The simultaneous appearance of the 1 1 0 and 0 0 1 types of superlattice reflection and their splitting in the SAED pattern result from the formation of three orientation variants of the AuCu I′ and AuCu II′ platelets, as observed in Fig. 9a, b and c. The α_2' phase is distinguished by a block-like configuration enclosed by metastable ordered platelets as seen in Fig. 9c. This situation is more clearly visible in Fig. 10 which is taken from a specimen aged at 648 K for 10 ks. In the dark-field image formed by using the 0 0 1-type superlattice reflection (for convenience,

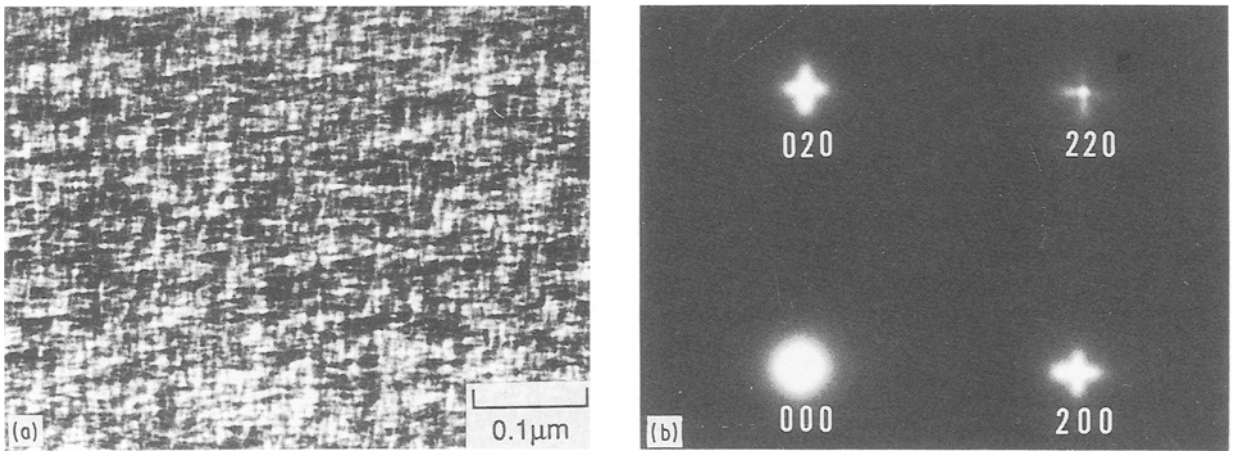

Figure 7 TEM image and SAED pattern taken from specimen aged at 773 K for 3×10^2 s: (a) dark-field image in the 2 2 0 fundamental reflection and (b) SAED pattern corresponding to (a).

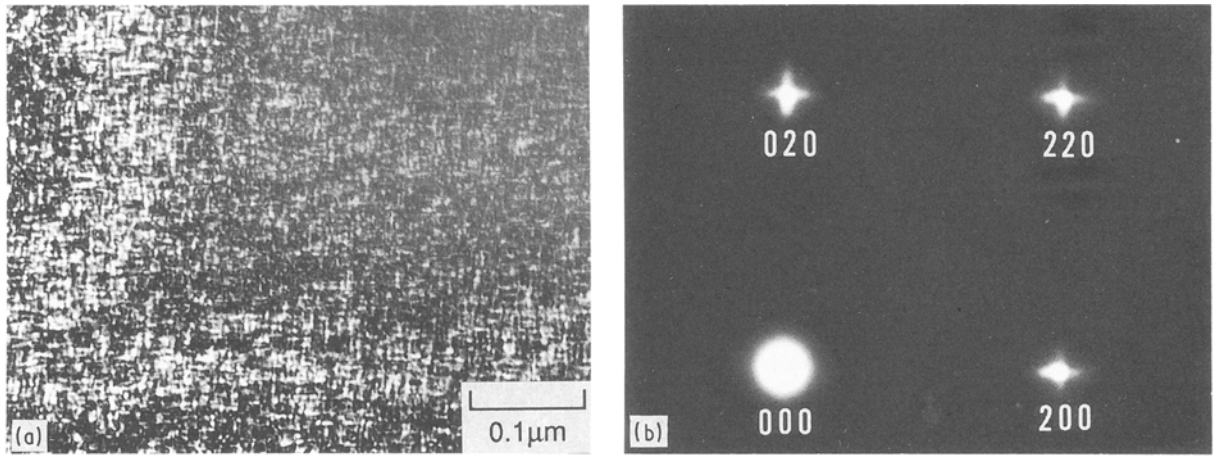

Figure 8 TEM image and SAED pattern taken from specimen aged at 573 K for 1×10^2 s: (a) dark-field image in the 220 fundamental reflection and (b) SAED pattern corresponding to (a).

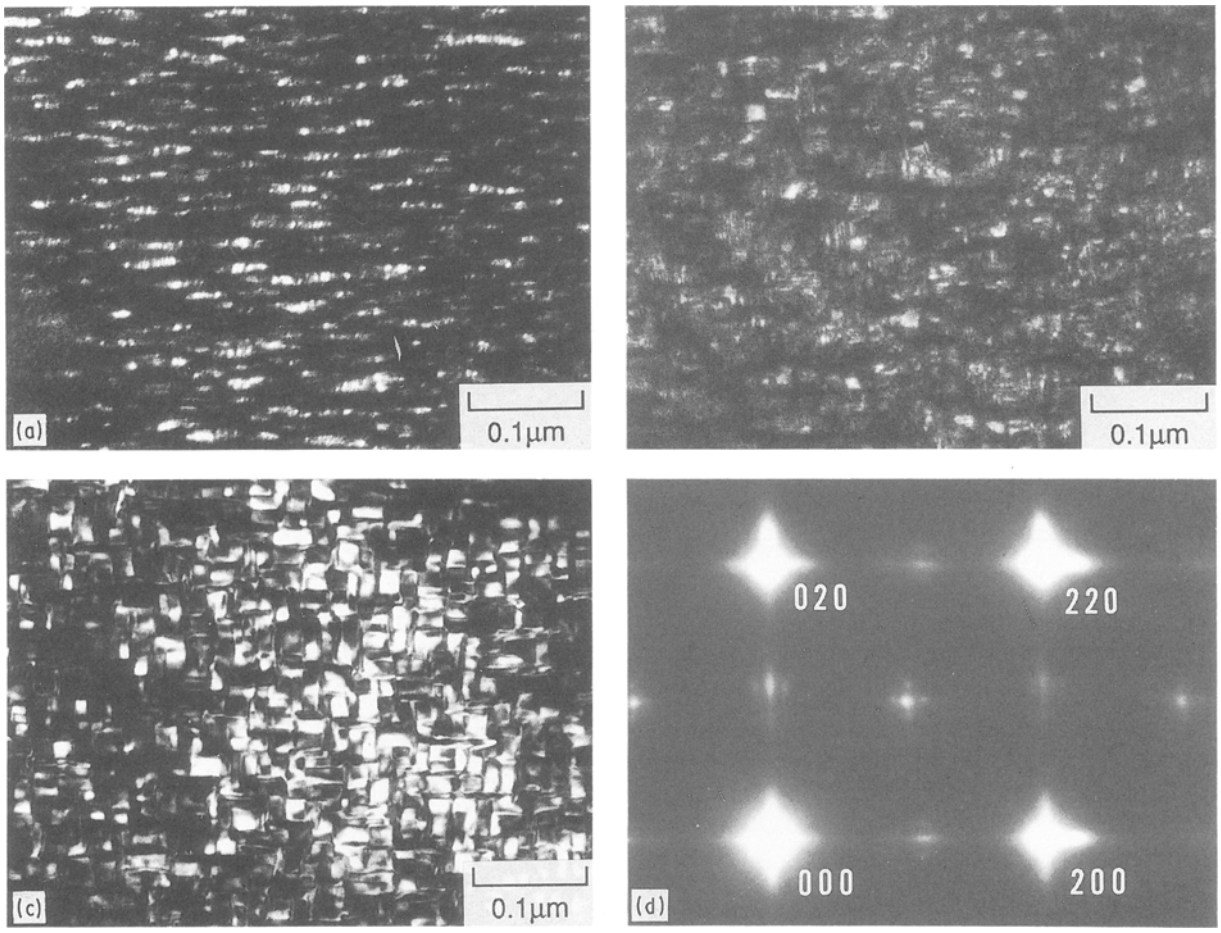

Figure 9 TEM images and SAED pattern taken from specimen aged at 573 K for 10 ks: (a, b) dark-field images in the 001 and 110 superlattice reflections, (c) dark-field image in the 220 fundamental reflection and (d) SAED pattern corresponding to (a–c).

Miller indices are used in terms of the AuCu I ($L1_0$) ordered tetragonal lattice), the ordered platelets are arranged at a wide interval along to the [0 1 0] direction as seen in Fig. 10a. By inspection of Fig. 10b and c, it can be concluded that the block-like configuration consisted of the α'_2 phase and thin platelets of the AuCu II′ formed alternately on the {1 0 0} planes in spite of the transitional ordering generated in this temperature range.

4. Discussion

The isothermal age-hardening behaviour of the present alloy showed a two-stage hardening by ageing below 648 K, whereas no hardening was observed at 773 K as seen in Fig. 2. This fact suggests that the age-hardening is brought about by overlapping of several phase transformations by ageing below 648 K.

Table I gives a summary of the present X-ray diffraction study. Although the occurrence of spinodal

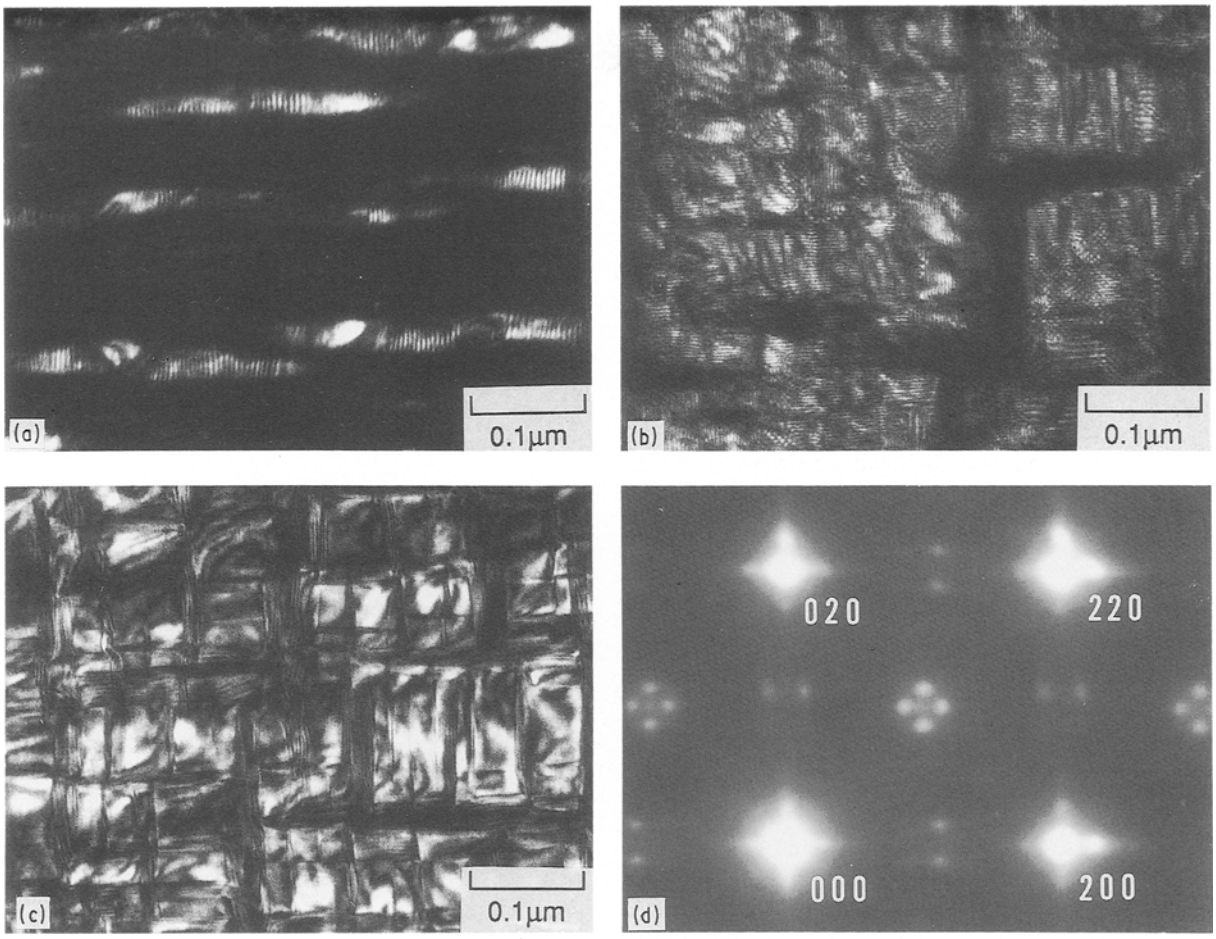

Figure 10 TEM images and SAED pattern taken from specimen aged at 648 K for 10 ks: (a, b) dark-field images in the 0 0 1 and 1 1 0 superlattice reflections, (c) dark-field image in the 2 2 0 fundamental reflection and (d) SAED pattern corresponding to (a–c).

TABLE I Summary of the phase transformation sequence obtained from the X-ray diffraction study

Temperature	Metastable phases	Stable phases
523	AuCu I′ + α_2'	AuCu I + α_2
573	AuCu I′ + AuCu II′ + α_2'	AuCu II + α_2
603	AuCu I′ + AuCu II′ + α_2'	AuCu II + α_2
623	AuCu I′ + AuCu II′ + α_2'	$\alpha_1 + \alpha_2$
648	AuCu II′ + α_2'	$\alpha_1 + \alpha_2$
773	–	$\alpha_1 + \alpha_2$

decomposition is not indicated in Table I, we can find several distinct phase transformation sequences including the transitional ordering process.

When the alloy was aged at 773 K for an extended period, there was no hardening. Notwithstanding the X-ray diffraction study showing that a two-phase decomposition solely took place, the SAED pattern and the dark-field TEM image showed characteristic side-maxima around the fundamental reflections along the ⟨1 0 0⟩ directions and cross-hatched contrast making traces parallel to the ⟨1 0 0⟩ directions, respectively. Thus, it was concluded that the modulated structure was brought about by spinodal decomposition during the early stage of ageing at 773 K. It was reported that hardening associated with the modulated structure came from internal strain, since formation of a modulated structure gave rise to an elastic strain field with the periodicity of the modulation [1, 5, 6]. In the present case, it was thought that the modulated structure gave rise to a small elastic strain field to introduce hardening because of small fluctuations of composition between the copper-rich and silver-rich portions, since the miscibility gaps moved in close to each other at this temperature. The lattice parameters of the α_1 and α_2 phases were found to be $a(\alpha_1) = 0.3879$ nm and $a(\alpha_2) = 0.4034$ nm, respectively.

When ageing was carried out below 648 K, the first hardening stage was generated by association with the modulated structure resulting from spinodal decomposition [1, 5, 6]. The second hardening stage was attributed to formation of the metastable AuCu I′ and/or AuCu II′ ordered phases, depending on the ageing temperature. These ordered phases were formed by ordering from the copper-rich portion of the modulated structure with a continuous mechanism. The silver-rich portion altered to the metastable α_2' phase with f.c.c. structure. The microstructural configuration of a specimen aged at 573 K for 10 ks showed a block-like mosaic structure [7] of the α_2' phase, enclosed by three orientation variants of the AuCu I′ and/or AuCu II′ ordered platelets formed alternately on the {1 0 0} planes [8], as seen in Fig. 9. Although it is thought that the α_2' phase acts as a buffer for the elastic strain induced by the tetragonality of ordered platelets, there is no doubt a large

amount of strain field which gives rise to hardening at the interface between the α'_2 and ordered phases. By prolonged ageing at 573 K, the stable AuCu II and α_2 phases were formed by a discontinuous mechanism. The lattice parameter of the α_2 and AuCu II ordered phases were found to be $a = 0.4072$ nm and $a = 0.3936$ nm with an axial ratio of $c/a = 0.94$ and antiphase domain size of $M = 5.0$, respectively.

In Fig. 2, a drastic decrease in hardness was observed in specimens aged at 623 and 648 K for lengthy periods. This softening coincided with decomposition of the metastable AuCu I′ and AuCu II′ ordered phases as indicated in Fig. 6. In other words, significant hardening was attributed to the transitional ordering which induced temporary formation of the metastable AuCu I′ and AuCu II′ ordered phases in the temperature range 623–678 K in spite of the temperature being higher than the critical temperature, $T_c = 620$ K, of ordering in the present alloy.

Occurrence of the transient ordering is explained by taking into consideration the free energy versus composition (ΔG–C) curves in the temperature range 623–648 K. If the ΔG–C curve is drawn on the tie-line for the present alloy at 648 K as shown in Fig. 11, the free energy of a supersaturated solid solution decreases along the curve as X_0–$A_1 + B_1$ in the early stage of ageing. Because the ΔG–C curve has a concave-downwards part which corresponding to a negative value of the second differential $(\partial^2 \Delta G/\partial C^2)$, the supersaturated solid solution tends towards spinodal decomposition. During the course of the phase separation, a metastable ordered phase and disordered phase appear at A_2 and B_2, respectively, since the A_2 point lies on the ΔG–C curve for the ordered phase. When the common tangential line contacts the points A_3 and B_3, giving the equilibrium phases, the ΔG–C curve for the ordering has already been detached from the common tangential line.

Thus spinodal decomposition occurred, followed by the metastable ordered phase, and disappeared finally during ageing.

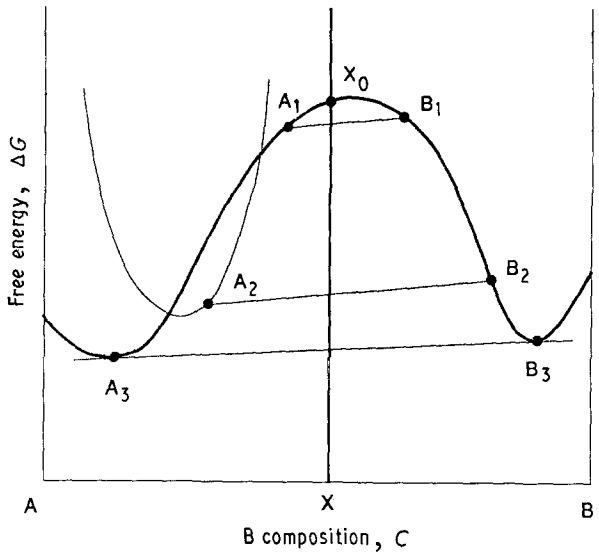

Figure 11 Schematic representation of free energy versus composition (ΔG–C) curve on the tie-line section at a temperature above T_c for the present alloy. The thick line is the ΔG–C curve for two-phase decomposition and the thin line corresponds to the ΔG–C line for metastable ordering.

Acknowledgement

The authors gratefully acknowledge the financial support of this work by the Japanese Ministry of Education, Science and Culture, Grant-in-Aid for Scientific Research (B) (01 460 241).

References

1. K. YASUDA and M. OHTA, in Proceeding of 3rd Conference on Precious Metals, Chicago, May 1979, edited by M. E. Browning (International Precious Metals Institute, New York, 1979) p. 137.
2. K. YASUDA and M. OHTA, *J. Dent. Res.* **61** (1982) 473.
3. M. NAKAGAWA and K. YASUDA, *J. Mater. Sci.* **23** (1988) 2975.
4. C. JOHANSSON and J. LINDE, *Ann. Physik* **25** (1936) 1.
5. T. J. TIEDEMA, J. BOUMASN and W. G. BURBERS, *Acta Metall.* **5** (1957) 310.
6. L. J. van DERTOORN, *ibid.* **8** (1960) 715.
7. M. OHTA, T. SHIRAISHI, M. YAMANE and K. YASUDA, *Dent. Mater. J.* **2** (1983) 10.
8. M. NAKAGAWA and K. YASUDA, *J. Less-Common Metals* **138** (1988) 95.

Received 20 September 1990
and accepted 7 March 1991